UC Berkeley

UC Berkeley Previously Published Works

Title

Subsoil particulate organic matter is more responsive to ~10 years of whole-soil warming than mineral-associated organic matter in a temperate forest

Permalink

https://escholarship.org/uc/item/3z1925x3

Journal

The Soil, 12(2)

ISSN

2151-1268

Authors

Sun, Binyan

Wiesenberg, Guido LB

Pegoraro, Elaine

et al.

Publication Date

2026-07-13

DOI

10.5194/soil-12-757-2026

Copyright Information

This work is made available under the terms of a Creative Commons Attribution License, available at https://creativecommons.org/licenses/by/4.0/

Peer reviewed

eScholarship.org Powered by the California Digital Library
University of California

SOIL, 12, 757–771, 2026
https://doi.org/10.5194/soil-12-757-2026
© Author(s) 2026. This work is distributed under
the Creative Commons Attribution 4.0 License.

SOIL Open Access EGU

Subsoil particulate organic matter is more responsive to ∼10 years of whole-soil warming than mineral-associated organic matter in a temperate forest

Binyan Sun[1], Guido L. B. Wiesenberg[1], Elaine Pegoraro[2], Margaret S. Torn[2], Michael W. I. Schmidt[1], and Mike C. Rowley[1]

[1]Department of Geography, University of Zurich, Zurich, Switzerland
[2]Earth and Environmental Sciences Area, Lawrence Berkeley National Laboratory, Berkeley, California, USA

Correspondence: Binyan Sun (binyan.sun@geo.uzh.ch) and Mike C. Rowley (mike.rowley@geo.uzh.ch)

Received: 5 November 2025 – Discussion started: 14 November 2025
Revised: 17 April 2026 – Accepted: 22 May 2026 – Published: 13 July 2026

Abstract. Global average temperatures are forecast to increase by 4 °C by 2100 under the Intergovernmental Panel on Climate Change SSP5-8.5 scenario. This warming could accelerate soil organic carbon (SOC) mineralization, net loss of soil carbon to the atmosphere, and consequently exacerbate global warming through a positive feedback loop. It is generally assumed that mineral-associated organic matter (MAOM) stocks are less sensitive to warming compared to particulate organic matter (POM), especially in the subsoil; yet more empirical data investigating the whole-soil responses to warming is still required to rigorously test this assumption.

Our study was conducted in a whole-soil field warming experiment in a temperate mixed-conifer forest at Blodgett Forest Research Station, University of California, Berkeley, which had been subjected to 9.5 years of warming. Soils from three depths (10–20, 40–50, and 80–90 cm) were separated into three density fractions, free POM (fPOM), occluded POM (oPOM), and MAOM. We then investigated the SOC concentration and composition of bulk soil and fractions with elemental analysis and diffuse reflectance infrared Fourier transform (DRIFT) spectroscopy. In subsoils below 50 cm, a decade of experimental warming caused bulk carbon loss and shifted its composition towards lignin and C–H aromatic bonds. Warmed plots had significantly lower mass of the POM fractions relative to control plots in the deep soil (80–90 cm) with no significant difference at or above 50 cm. fPOM composition showed a significant shift towards enrichment in lignin at 40–50 cm but not in topsoils. Meanwhile, MAOM mass and composition shifted along the depth gradient but were not significantly affected by warming. This study at Blodgett Forest thus supports the assumption that POM will be more responsive to warming in the subsoil than MAOM.

1 Introduction

Soil is the largest actively-cycling terrestrial carbon reservoir, storing more carbon than the atmosphere and vegetation combined (Jackson et al., 2017; Scharlemann et al., 2014; Schlesinger, 1990). Under the SSP5-8.5 scenario, global temperatures are projected to increase by 3.3–5.7 °C by 2100 (IPCC, 2023). This warming could accelerate the decomposition of soil organic carbon (SOC) and increase soil carbon dioxide (CO_2) fluxes (Davidson and Janssens, 2006; Schlesinger and Andrews, 2000). Warming-induced soil CO_2 fluxes could further exacerbate global warming, creating a positive feedback cycle (Davidson and Janssens, 2006). Many studies have examined SOC responses to warming and reported variable outcomes, ranging from no net cumulative changes (Giardina et al., 2014; Lu et al., 2013) to large SOC losses observed in more recent field warming experiments (Nottingham et al., 2020; Soong et al., 2021; Verbrigghe et al., 2022). The contrasting results reflect the differences in experimental approaches as well as the complexity of soil systems, where opposing mechanisms simultaneously influence SOC inputs and decomposition. As a result, bulk soil

measurements alone can lack the sensitivity needed to uncover the processes driving SOC responses (Lavallee et al., 2020; Rocci et al., 2021). Instead, investigating how fractions of soil, each with distinct physical and chemical properties, respond to warming could improve our understanding of the key mechanisms that govern SOC dynamics (Georgiou et al., 2022; Lugato et al., 2021).

Soil organic carbon is typically operationally-divided by size or density fractionation into two main fractions, particulate organic matter (POM) and mineral-associated organic matter (Lavallee et al., 2020). In turn, POM can be further separated into free particulate organic matter (fPOM) and occluded particulate organic matter (oPOM); where, fPOM consists of partially-decomposed fragments of plant biomass stored freely within the soil, and oPOM consists of plant fragments that are enclosed within soil aggregates, separated after physical disturbance (Golchin et al., 1994; von Lützow et al., 2006). Carbon in MAOM includes both plant-derived biomolecules (Angst et al., 2021) and microbial-derived products such as necromass and metabolites (Lehmann and Kleber, 2015; Sanderman et al., 2014; Sollins et al., 1999). Due to its strong association with minerals, MAOM is considered less accessible to decomposers or their extra cellular enzymes, and consistently has longer turnover times (Heckman et al., 2022; Kaiser and Guggenberger, 2000; Lavallee et al., 2020; von Lützow et al., 2006). Therefore, it is also often assumed to be more resistant to warming-enhanced decomposition than POM fractions (Georgiou et al., 2024; Williams et al., 2018). Nevertheless, there is limited empirical evidence to support or refute this assumption (Guan et al., 2018; Schnecker et al., 2016) and few studies have investigated how the distribution of SOC amongst these fractions changes with warming (Chen et al., 2023; Schnecker et al., 2016; Soong et al., 2021).

Warming can influence not only SOC concentration and its distribution among physical fractions but also its chemical composition (vandenEnden et al., 2021). SOC is composed of a diverse array of biopolymers at varying stages of decay along a continuum within the soil profile, containing different organic functional groups (Kleber et al., 2021; Lehmann and Kleber, 2015). SOC functional groups are specific arrangements of atoms within organic molecules that differ in their charge and reactivity, therefore influencing their potential for mineral association (Kögel-Knabner, 2002; von Lützow et al., 2006). Oxygen-containing functional groups such as carboxyl functional groups can strongly bind to metal (oxyhydr)oxide surfaces through ligand exchange reactions (Kleber et al., 2021; Rowley et al., 2025; Spohn, 2024). Warming induced shifts in the relative abundance of SOC functional groups may therefore alter the strength and mechanisms of MAOM formation, influencing SOC stabilization and persistence (Xu and Tsang, 2024). However, exactly how warming affects SOC composition throughout the entire soil profile remains poorly understood.

Whole-soil warming experiments have been instrumental in advancing our understanding of the response of SOC to warming, particularly in subsoils (> 30 cm), which are estimated to contain ∼ 50 % of SOC globally (Jobbágy and Jackson, 2000). Although subsoil SOC is postulated to be resistant to warming (Harrison et al., 2011), its responses to warming remain largely uncertain. The Blodgett Forest whole-soil warming experiment has been investigating how the top meter of soil of a temperate mixed-conifer forest responds to +4 °C warming. Studies have thus far demonstrated that 4.5 years of +4 °C warming at Blodgett Forest promoted decomposition and SOC loss in subsoils (Hicks Pries et al., 2017; Soong et al., 2021), reduced fine-root biomass, and accelerated decomposition of biochemically-complex SOC (Ofiti et al., 2021; Zosso et al., 2023). Specifically, the SOC loss in the subsoil at Blodgett Forest after this short-term warming was driven by a reduction in POM, while MAOM stocks remained largely unaffected (Soong et al., 2021). Given the paucity of fresh plant inputs to deeper horizons, subsoil POM losses are less likely to be replenished (Button et al., 2022; Hicks Pries et al., 2023; Jackson et al., 1996). If subsoil POM losses persist over decadal timescales, the resulting lower POM availability could limit microbial processing and in turn, constrain further MAOM formation derived from microbial transformation of POM (Heckman et al., 2022; Witzgall et al., 2021). However, it remains unclear how prolonged warming will affect the balance between POM and MAOM and their composition at deep-soil warming experiments such as Blodgett Forest and whether these SOC losses in individual fractions persist or stabilize over decadal timescales.

To address this knowledge gap, we investigated responses in the distribution of SOC and its composition across fractions and depths after 9.5 years of warming at Blodgett Forest. We fractionated soil from soil cores using density fractionation separating fPOM, oPOM, and MAOM fractions. We quantified bulk soil and fraction carbon concentration, stable carbon isotope composition (δ^{13}C values), and characterized their chemical composition using diffuse reflectance infrared Fourier transform (DRIFT) spectroscopy. We hypothesized that at 10–20 and 40–50 cm, warming would not cause substantial quantitative losses of SOC fractions because continued fresh plant inputs would offset carbon losses. Accordingly, we expected compositional changes at these depths to be limited. In contrast, in deep subsoils (80–90 cm), we expected fPOM and oPOM to decline quantitatively under warming, whereas MAOM would remain comparatively stable. We further hypothesized that warming would shift fPOM towards relatively more aromatic signals as labile aliphatic C–H and polysaccharide components were preferentially depleted. By contrast, we expected no significant warming effect on oPOM and MAOM composition throughout the soil profile because of their inherent heterogeneity (Marín-Spiotta et al., 2008; Schrumpf et al., 2013) and resistance, respectively.

2 Materials and methods

2.1 Study site and sampling

The whole-soil warming experiment is located in the Blodgett Forest Research Station, of the University of California, Berkeley, in the foothills of the Sierra Nevada near Georgetown, California (38°54′43.0″ N 120°39′40.0″ W; 1370 m a.s.l. – above sea level). The climate is characterized as Mediterranean with a mean annual air temperature of 12.5 °C and a mean annual precipitation of 1774 mm yr^{-1}, falling predominantly between November through April (Hicks Pries et al., 2017). The experiment is located in a mixed coniferous forest dominated by ponderosa pine (*Pinus ponderosa*), sugar pine (*Pinus lambertiana*), incense cedar (*Calocedrus decurrens*), white fir (*Abies concolor*), and Douglas fir (*Pseudotsuga menziesii*; Hicks Pries et al., 2017). The understory vegetation mainly consists of shrubs (*Notholithocarpus densiflorus*), grasses, and annual plants such as *Gallium triflorum*. The soil is a mesic ultic Alfisol of granitic origin, which is equivalent to a Dystric Cambisol (IUSS Working Group WRB, 2022), with fine-loamy texture.

The warming experiment started in January 2014 with three pairs of control and warmed treatment plots, as described by Hicks Pries et al. (2017). The control and treatment plots have the same experimental set up. Briefly, each 3 m diameter plot is surrounded by 22 conduit pipes installed vertically down to 2.4 m. In warmed plots, these conduits contain heating cables. Each warmed plot has two concentric rings of surface heating cable, while control plots have plain wire installed 5 cm below the surface. The temperature in each warmed plot was elevated by +4 °C compared to its paired control plot. In May 2023, two cores from each plot were collected in 10 cm depth increments down to 1 m depth. Samples were stored at −4 °C until processing.

2.2 Soil preparation

Samples were sieved to 2 mm to separate the fine-soil fraction (< 2 mm), removing large rock fragments and roots. Tweezers were used to manually remove roots from the fine-soil fraction that passed the sieve. The soil samples were then freeze-dried to a constant weight. Before laboratory analysis, sub-samples from identical depth increments of the two different cores from the same plot were combined to obtain a more representative bulk sample in an effort to account for within–plot variability. A subset of these combined samples was then ground with a ball mill (MM400, Retsch, Haan, Germany) for elemental analysis.

Topsoil and subsoil will refer to soil between 0–30 and 30–100 cm, respectively. Surface soil, mid-depth soil, and deep soil will respectively refer to the soil depth of 10–20, 40–50, and 80–90 cm throughout the Results and Discussion sections.

2.3 Density fractionation

Bulk soil samples from three depths (10–20, 40–50, and 80–90 cm) were fractionated by density into free POM (fPOM, large undecomposed or partially decomposed plant fragments), occluded POM (oPOM, plant fragments released by sonication), and MAOM (residual SOC bound to minerals) fractions in sodium polytungstate solution (SPT), with methods adapted from a previous study of this site (Hicks Pries et al., 2018). Like previous studies at this site (Hicks Pries et al., 2018; Soong et al., 2021), we used an SPT density of 1.65 g cm^{-3}. The three depths were selected because they represented different soil horizons and permitted a comparison with previous analyses at the same experiment site, which used the same depths (Hicks Pries et al., 2017; Soong et al., 2021).

We conducted fractionation in an 80 mL round bottom glass centrifuge tubes (Neubert-Glas, Germany) to avoid potential plasticizer contamination for subsequent lipid analysis. Briefly, 40 mL of 1.65 g cm^{-3} low C and N content SPT (SPT0, TC-Tungsten Compounds Inc., Grub am Forst, Germany) were added to 8 g bulk soil in a round-bottom glass centrifuge tube with four analytical replicates per sample. The glass tube was gently shaken by hand to enable full contact between the soil particles and the solution, ensuring that particles adhering to the tube walls were brought back into solution. We let the samples stand for 1 h to allow for density equilibration and maximize the separation of fPOM from MAOM before centrifuging the solutions in a swinging bucket rotor for 1 h at 3130 RCF (Megafuge 1.0, Heraeus Group, Germany). The fPOM was aspirated using a 10 mL Eppendorf pipette, filtered through a 0.8 µm polycarbonate filter (Nucleopore Track-Etch, Whatman), and rinsed with deionized water (Millipore MilliQ Advantage A10, Darmstadt, Germany, 18.2 MΩ cm^{-1} at 25 °C). The remaining sample was then sonicated in an ice bath at maximum amplitude and a 50 % pulse rate for 2 min and 26 s, delivering a calibrated (North, 1976) total energy input of 100 J mL^{-1} (Hicks Pries et al., 2018). The sample was then centrifuged, again at 3130 RCF for 1 h and left to settle overnight. Subsequently, the same aspiration and rinsing procedure used for fPOM was applied to the floating material, fractionating the oPOM. To prevent the re-adsorption of oPOM onto the MAOM and ensure complete removal of oPOM, the remaining mixture was centrifuged (3130 RCF for 1 h), aspirated, filtered, and rinsed a second time. All fractions, including the MAOM, the remaining solid sample recovered in the tube, were then rinsed with deionized water until the supernatant reached the density of water. All fractions were freeze-dried at −50 °C (Alpha 1–4, Martin Christ Freeze Dryers, Osterode am Harz, Germany). Then a subsample of fPOM and oPOM were ground by hand with a pestle and agate mortar and a subsample of MAOM was ground with a ball mill (MM400, Retsch, Haan, Germany) for elemental and DRIFT analysis.

2.4 Carbon and nitrogen concentrations and carbon stable isotope compositions

Soil organic carbon concentrations (C %) and stable carbon isotope compositions (δ^{13}C values) were analyzed in bulk soils and fractions using an elemental analyzer-isotope ratio mass spectrometer (EA–IRMS; Flash 2000–HT Plus, linked by Conflo IV to Delta V plus isotope ratio mass spectrometer, Thermo Fisher Scientific, Bremen, Germany). Caffeine (Merck, Germany) and Chernozem standards (Harsum, Germany) were used as calibration materials. δ^{13}C values were expressed in ‰ relative to the Vienna Pee Dee Belemnite (VPDB) standard (Coplen, 2011). At least two analytical replicates were measured for all samples. A previous study measured the pH values at the same study site (Rowley et al., 2025). The soils are acidic and have a pH (H_2O) of 4.9 ± 0.1 (standard error of the mean), ranging between extremely and slightly acidic (3.7–6.2). Thus, carbonates are absent at Blodgett Forest, so total carbon concentrations are assumed to represent SOC concentrations.

2.5 SOC composition analysis

To assess potential differences in SOC composition between treatments and across soil depths in both bulk soil and fractions, ground bulk and fraction samples were analyzed using DRIFT spectroscopy. A Bruker Invenio R spectrometer (Billerica, Massachusetts, USA) was used to record the mid-infrared spectra with a resolution of $2\,cm^{-1}$ between 4000 and $80\,cm^{-1}$, collecting 64 scans for each sample. Background reflectance was determined on oven-dried KBr (60 °C) and subtracted to convert spectra to pseudo-absorption units (log[1/R]). Background-corrected scans were checked for consistency and then averaged to produce a single spectrum.

All subsequent spectral processing was completed in R version 4.4.2 (R Core Team, 2025) using the "*prospectr*" (v0.2.8; Stevens and Ramirez-Lopez, 2025) and "*tidyverse*" (v1.3.2; Wickham et al., 2019) packages. Briefly, spectra were concatenated into a single datafile and trimmed to between 4000–$400\,cm^{-1}$ to remove spectral noise. Prior to standard normal variate normalization (SNV), the data was smoothed using a Savitzky–Golay filter to the 3rd order polynomial (Savitzky and Golay, 1964) and scaled to positive values (Fearn, 2008). SNV was applied to the spectra to eliminate scattering effects and standardize spectral intensities, before applying a convex-hull rubber-band baseline correction. Area under the curve (AUC) of spectral peaks was calculated using a trapezoid area function with local baseline calculation, to ascertain the area of peaks linked to different bonding environments of SOC. The spectral band ranges assigned to different carbon functional groups were based on previous studies (Artz et al., 2008; Chatterjee et al., 2012; Ofiti et al., 2021) and are reported in Table S13. The average AUC plot for each sample type (fPOM/oPOM or bulk/-MAOM) was calculated and used to minimally adjust the wavenumber range of spectral bands for each peak due to slight spectral shifts caused by the mineral matrix (Table S13; Ellerbrock and Gerke, 2021).

The ratio of peak areas between aromatic C=C/carboxylic C=O stretches (in our paper assigned as C=C aromatic2; Table S13) and aliphatic C–H stretches was used to calculate the DRIFT Stability Index (DSI; Demyan et al., 2012; Haberhauer et al., 1998; Laub et al., 2020; Schiedung et al., 2025), used as a proxy of the relative state of SOC decomposition. In soils devoid of carbonates such as Blodgett forest, the band range at ~ 3000–$2800\,cm^{-1}$ is largely unaffected by mineral-phase interference (Tinti et al., 2015). Other confounding influences on the spectra should be minimal because we always compare samples collected from close proximity with a similar parent material and texture (Reeves, 2012). We could not conduct DRIFT analysis on several POM fractions from the deep soil due to the limited amount of material recovered, particularly in fractions from warmed plots.

2.6 Statistical analysis

All statistical analyses were performed in R version 4.4.2 (R Core Team, 2025) using Rstudio (2024.12.1.563; Posit team, 2024). Plots were all created using the "*ggplot2*" (v3.5.1; Wickham, 2016) and "*ggbiplot*" packages (v0.6.2; Vu and Friendly, 2024). To test the effect of depth, treatment, and their interaction on bulk SOC concentration, δ^{13}C values, AUC values for each bond type, and the DSI, we built linear mixed effects models in the "*nlme*" package (v3.1.166; Pinheiro and Bates, 2000; Pinheiro et al., 2025). We set depth, treatment, and their interaction as fixed effects, setting the plot pair as a random effect. Model fits were assessed using Akaike's Information Criterion (Akaike, 1998). To account for autocorrelation of observations within profiles, depth class was set as a repeated measure with an autoregressive (AR1; "*nlme*") covariance structure (Grand et al., 2014). Homoscedasticity of residues were visually examined using conditional residual plots (Zuur et al., 2009) and normality was assessed using Q–Q plots. If model assumptions were not met, as was only the case with SOC concentration and AUC values, the data were log-transformed.

For fractions, we applied linear mixed effects models to the three fractions separately. We tested the effects of depth, treatment, and their interaction on SOC concentration in each fraction ($mg\,C\,g^{-1}$ fractionated soil), distribution of C in the density fractions ($g\,C\,fraction\,g^{-1}$ bulk SOC), AUC values, and DSI. Plot pairs were again set as a random effect. When significant fixed-interaction effects were discovered, we ran post hoc analyses within each depth increment. The alpha level was set to $\alpha = 0.05$ in all statistical tests, where a $p < 0.05$ was reported as significant and a p between 0.05–0.1 as marginally significant.

To further explore trends in the bulk soil and fraction SOC composition, AUC values from the DRIFT spectra were analyzed using principal component analysis (PCA). The PCA was performed on the correlation matrix, centered and scaled using "*prcomp*" in the R "*stats*" package (v4.4.2; R Core Team, 2025). We used 95 % confidence ellipses to visualize the approximate location of the true group centroids (mean) and the dispersion of different groups within Euclidean space (Husson et al., 2005).

3 Results

3.1 Bulk soil SOC properties

Independent of treatment, SOC concentration significantly declined with depth ($p < 0.001$; Table 1). Warming reduced SOC concentration in the soil samples from 50–100 cm, but not in the samples between 0–50 cm ($p = 0.002$; Table 1). Specifically, at 60–70 and 80–90 cm, mean SOC concentrations were on average 54 % (CI: −83, 26) and 56 % (CI: −84, 20) lower, respectively; but, the wide confidence intervals and marginally significant p values in the post-hoc tests (0.099 and 0.086, respectively) indicate substantial variability rather than a definitive loss. There was no significant effect of warming on bulk SOC δ^{13}C values ($p > 0.1$; Table 1) but these values significantly decreased with depth ($p < 0.001$).

3.2 In deep soil, fPOM concentration was more responsive to warming than was MAOM

fPOM concentrations significantly declined with depth ($p < 0.001$), and a significant interaction effect between depth and treatment was also observed ($p = 0.031$), meaning the effect of warming varied across depths (Fig. 1). Specifically, warming had a negative effect on fPOM concentrations in deep soils (80–90 cm), marginally reducing it by 70 % (CI: −91, 2.0; $p = 0.053$). oPOM organic carbon (OC) concentrations also significantly decreased with depth ($p < 0.001$) and the interaction effect between warming and depth was marginally significant ($p = 0.082$). At 10–20 and 40–50 cm, there was no significant difference in oPOM concentrations between control and warmed plots. However, warming significantly decreased oPOM concentrations at 80–90 cm, reducing its concentration by 80 % (CI: −95, −25; $p = 0.022$). MAOM concentrations displayed a significant decline across soil depth ($p < 0.001$), but in contrast to fPOM and oPOM fractions, warming had no effects on MAOM concentrations ($p > 0.1$).

The proportions of fPOM relative to total SOC were not significantly affected by warming ($p > 0.1$) but significantly decreased with depth ($p = 0.002$). The average values ranged from 0.11–0.49 g C g^{-1} bulk SOC in warmed plots and 0.18–0.41 g C g^{-1} bulk SOC in control plots (Fig. 2). The proportion of oPOM relative to total SOC marginally decreased by depth ($p = 0.061$), driven by a significant decrease in oPOM proportions between the 40–50 and 80–90 cm samples of 0.07 g C g^{-1} bulk SOC (CI: −0.13, −0.01; $p = 0.022$; Fig. 2). The oPOM proportions were significantly affected by warming, independent of depth ($p = 0.027$; Fig. 2). Warming caused a reduction in the proportion of oPOM by 0.06 g C g^{-1} bulk SOC (CI: −0.11, −0.01) across the soil profile. The proportion of MAOM was not affected by warming ($p > 0.1$) but significantly increased with depth ($p = 0.001$). On average, the proportion of MAOM increased from 0.41–0.66 g C g^{-1} bulk SOC in control plots and from 0.38–0.81 g C g^{-1} bulk SOC in warmed plots across soil profile (Fig. 2).

3.3 Bulk SOC composition change

Bulk SOC composition changes with depth and between warmed and control plots are displayed in the PCA biplot (Fig. 3). The first two principal components explained 44.9 % (1st) and 19.4 % (2nd) of total variation in the bulk DRIFT AUC dataset (Fig. 3). SOC composition showed a strong depth-related pattern with samples moving along principal component 1 and topsoil samples (0–30 cm) were clearly separated from subsoil samples (> 30 cm). Topsoils did not cluster according to treatment and were associated with relatively high AUC values for aliphatic ($p < 0.001$) and C=C aromatic (range 1; $p < 0.001$) regions of the DRIFT spectra (Fig. 3). Samples from 30–40 cm depth contained relatively higher proportions of polysaccharide and carboxylic functional groups and showed no clear treatment-based separation. In contrast, at depth > 40 cm, subsoil samples tended to separate along principal component 2 according to treatment. Under warming, subsoils below 40 cm tended to shift from C=C aromatic (range 2) and C–H aromatic (range 2) to C–H aromatic (range 1) and lignin-like residues (Fig. 3). However, the large standard errors of average PCA scores for subsoil samples indicate substantial within-group variability (Fig. S1 in the Supplement), suggesting again, that these patterns should be interpreted as indicative trends with depth.

3.4 SOC compositional changes in soil density fractions

The PCA of POM fractions is displayed in the supplementary information (Fig. S2). Briefly, the main differences in POM composition were observed between the free and occluded POM fractions rather than with warming or depth. Although SOC in both fractions was composed primarily of aliphatic SOC (Table S7), oPOM contained proportionally more aliphatic carbon than fPOM. Warming tended to shift fPOM composition at 40–50 cm to lignin-like residues and aromatic C–H (range 2; Fig. S2), which was confirmed by significantly increased AUC values for lignin-like residues ($p = 0.002$) and marginally increased aromatic C–H AUC values (range 2; $p = 0.061$). fPOM in topsoils and oPOM

Table 1. Soil organic carbon (SOC) and stable carbon isotope compositions $\delta^{13}C$ values of mineral bulk soils (0–100 cm) in the control and warmed plots (mean ± SE) after 9.5 years of soil warming. $\delta^{13}C$ values are reported in ‰ relative to the Vienna Pee Dee Belemnite (VPDB) standard.

Depth	Control		Warmed	
[cm]	SOC [mg C g^{-1} soil]	$\delta^{13}C$ [‰ VPDB]	SOC [mg C g^{-1} soil]	$\delta^{13}C$ [‰ VPDB]
0–10	43.4 ± 4.7	−25.6 ± 0.2	42.9 ± 2.9	−25.6 ± 0.5
10–20	33.7 ± 6.5	−25.4 ± 0.2	46.7 ± 10.4	−25.6 ± 0.3
20–30	25.1 ± 5.8	−25.5 ± 0.1	40.6 ± 19.9	−25.5 ± 0.3
30–40	14.9 ± 3.4	−25.3 ± 0.1	21.4 ± 9.4	−25.3 ± 0.1
40–50	9.9 ± 2.6	−24.9 ± 0.1	10.8 ± 3.2	−25.1 ± 0.1
50–60	7.7 ± 1.6	−25.0 ± 0.1	5.7 ± 0.9	−25.0 ± 0.2
60–70	7.4 ± 1.1	−25.1 ± 0.3	3.5 ± 0.7	−24.6 ± 0.3
70–80	5.9 ± 1.4	−25.0 ± 0.3	2.8 ± 0.6	−24.6 ± 0.3
80–90	4.3 ± 1.4	−25.0 ± 0.3	1.8 ± 0.4	−24.9 ± 0.1
90–100	3.2 ± 0.6	−25.3 ± 0.5	2.0 ± 0.6	−25.0 ± 0.3

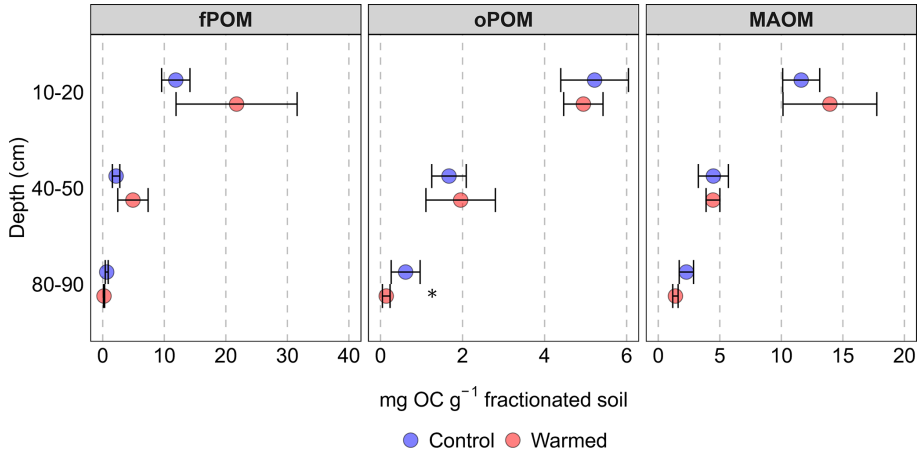


Figure 1. Soil organic carbon (SOC) concentration in each soil fraction (mg OC g^{-1} fractionated bulk soil) at three depths (10–20, 40–50, and 80–90 cm) in control and warmed plots ($n = 3$), error bars represent the standard error of the mean. The asterisks indicate the significant treatment effects ($p < 0.05$ "*"; < 0.01 "**") on the mass of SOC in the corresponding recovered fraction.

were not affected by either warming or depth (Fig. S2). However, warming tended to increase the variability of POM composition, as indicated by the broader dispersion of the fPOM and oPOM samples from warmed plots along the principal component 2 in the PCA plot (Fig. S2).

The first two principal components explained 48.6 % (1st) and 30.6 % (2nd) of the total variation in the fit DRIFT data of the MAOM fraction (Fig. 3). SOC composition in MAOM exhibited a depth-related trend along principal component 2, with MAOM at 10–20 cm relatively enriched in aliphatic and C=C aromatic (range 1) bonds, while those from 40–50 and 80–90 cm were more associated with lignin-like residues and C–H aromatic (range 2) bonds. Warming did not alter MAOM composition at individual depths but substantially increased the variability in its composition at 80–90 cm and exhibited a tendency shift from C–H aromatic (range 2) to lignin-like residues and aromatic C–H (range 1; Fig. 4).

3.5 No significant changes of aromatic/aliphatic ratio in bulk soil and fractions

We did not find significant effects of warming ($p > 0.1$), but significant effects of depth ($p < 0.001$; Fig. 5) on the DRIFT stability index (DSI) of bulk soils. Specifically, bulk soil DSI significantly increased with depth (Fig. 5).

There were no significant effects of warming and depth on the DSI of fPOM and oPOM ($p > 0.1$). On average, the fPOM DSI at 10–20 cm (0.27 ± 0.02) and 40–50 cm (0.18 ± 0.03) in warmed plots were lower relative to the values at corresponding depths in control plots (0.29 ± 0.07 and 0.23 ± 0.06 respectively for 10–20 and 40–50 cm). Similar to fPOM, oPOM DSI exhibited lower values at 10–20 cm

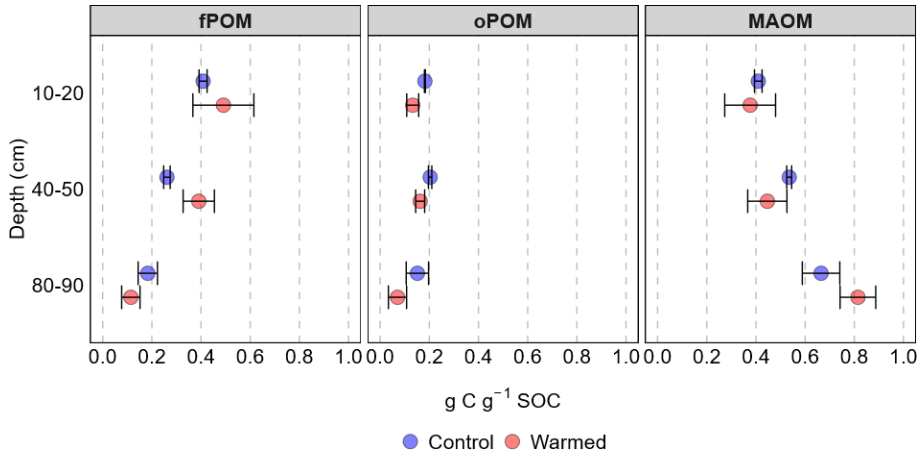


Figure 2. Distribution of total soil organic carbon (SOC) in the density fractions (g C g^{-1} total SOC) at three depths (10–20, 40–50, and 80–90 cm) in control and warmed plots (mean ± SE, $n = 3$).

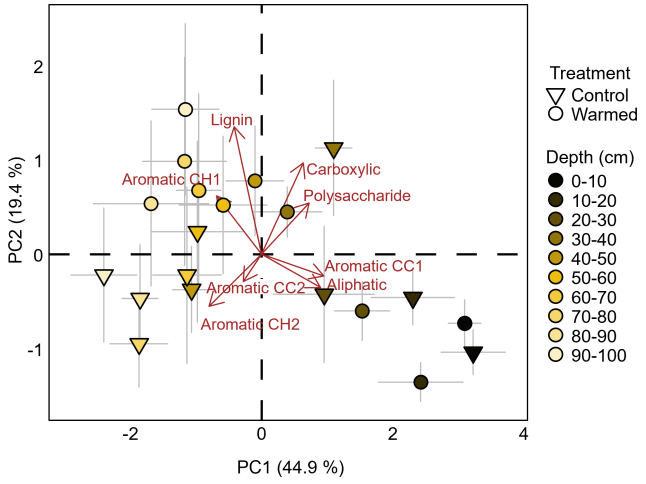


Figure 3. Principal component analysis (PCA) of the area under the curve (AUC) values from fit diffuse reflectance infrared Fourier transform spectra of bulk soil in control and warmed plots at 10 cm intervals from 0 to 100 cm. Each point represents the mean PCA scores of the three replicate samples per depth and treatment. The horizontal (PC1) and vertical lines (PC2) indicate the standard error of the mean of principal component scores for each plot type (control and warmed, $n = 3$), respectively. The number after aromatic C=C/aromatic C–H refers to the same C–bond type assigned at different band ranges (Table S13).

(0.18 ± 0.03) and 40–50 cm (0.14 ± 0.08) under warming compared to ambient temperature conditions (0.16±0.01 and 0.11 ± 0.02 at 10–20 and 40–50 cm, respectively; Table S9). However, these differences were subtle due to large standard errors.

MAOM DSI was not significantly affected by warming ($p > 0.1$), but it significantly increased with depth ($p < 0.001$). Although MAOM DSI was on average larger in warmed than in control plots at 80–90 cm, this difference was statistically indistinguishable from zero due to high variability within the data ($p > 0.1$; Fig. 5).

4 Discussion

4.1 Depth-specific shifts in SOC quantity and composition under long-term warming

4.1.1 Subsoil carbon loss to warming

There was a significant effect of depth and interaction between depth and treatment on SOC concentrations, which indicated that topsoils responded to 9.5 years of whole-soil experimental warming differently than subsoils (Table 1). This pattern of contrasting shallow versus deep responses in SOC concentration to warming is broadly consistent with earlier observations from the same site (Soong et al., 2021). However, the depth at which the warming response became evident was deeper in the more recent sampling campaign. In particular, the current study did not find a decline in SOC between 30–50 cm as was reported after 4.5 years of warming at this site (Soong et al., 2021; Zosso et al., 2021).

The shifts in depth of SOC-concentration decline between these two time points could be due to site heterogeneity or changes in rates and depths of plant inputs. Plant inputs to temperate forest soils at these depths are dominated by root inputs (Angst et al., 2016; Wordell-Dietrich et al., 2020). There was less root biomass in warmed than control plots at almost at every depth (except for 20–30 cm interval) after 4.5 years (Ofiti et al. 2021). Yet, modeling of the site suggests that root responses may attenuate over time as plants approach a new balance between growth and maintenance costs under long-term warming (Riley et al., 2025). Recent observations from another temperate forest soil-warming experiment support a time-varying response, as fine root biomass did not increase in the short-term (8 years), but increased significantly with over a decade (14 years) of

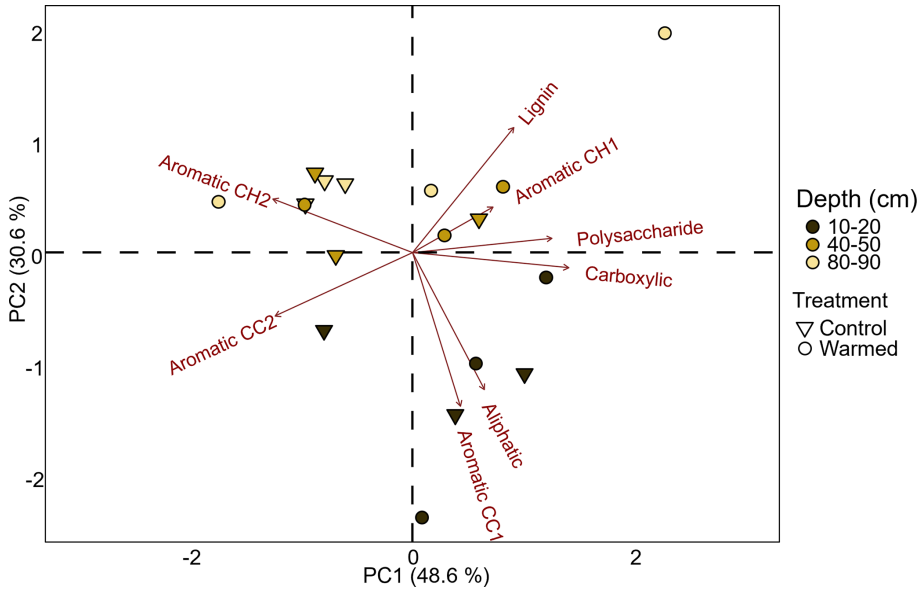


Figure 4. Principal component analysis (PCA) of area under the curve values from fit diffuse reflectance infrared Fourier transform spectra of MAOM from control and warmed plots at three depth intervals (10–20, 40–50, 80–90 cm). Each point represents the MAOM of one sample. The number behind aromatic C=C/aromatic C–H refers to the same carbon bond type assigned at different band ranges (Table S1).

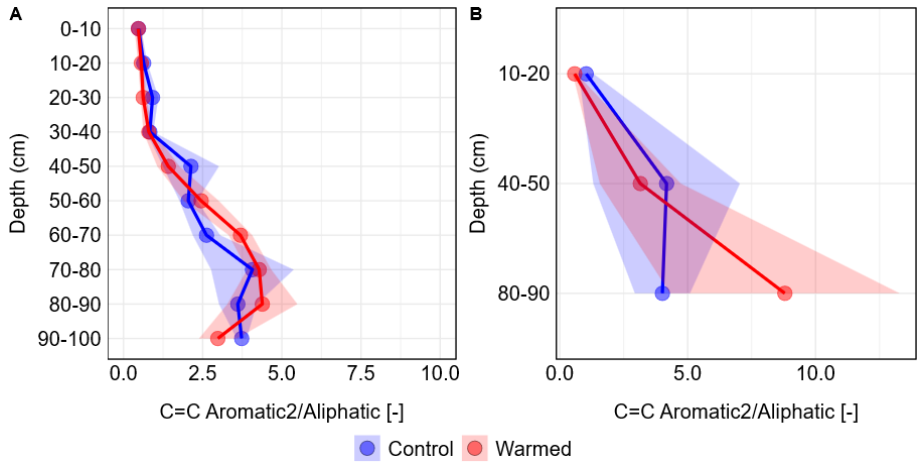


Figure 5. The diffuse reflectance infrared Fourier transform (DRIFT) spectral stability index (DSI) or ratio between area under the curve values (AUC) of C=C aromatic (range 2) to aliphatic in bulk soil **(A)** at 10 depth increments from 0 to 100 cm and MAOM **(B)** at three soil depths (10–20, 40–50, and 80–90 cm) under control and warmed conditions (mean ± SE, $n = 3$). The ratio (C=C aromatic2/aliphatic) was calculated using the AUC values corresponding to the aliphatic (3020–2800 cm^{-1}) and C=C aromatic (range 2; 1670–1600 cm^{-1}) regions. The ratios of POM fractions are shown in Table S9.

warming (Kwatcho Kengdo et al., 2022). We thus speculate that warming may have stimulated deeper root growth after 9.5 years of warming, compensating the loss of SOC concentrations in mid-depths (Table 1). Yet, this hypothesis requires further verification with additional depth-resolved root measurements.

Post-hoc tests revealed that warming marginally reduced SOC concentrations in subsoils below 50 cm, with the strongest declines at 60–70 and 80–90 cm (Table 1). The loss of subsoil carbon in this experiment highlights the vulnerability of deep SOC to long-term warming. However, we hypothesize that the initial stimulation of heterotrophic respiration could attenuate over time (Riley et al., 2025), for example due to microbial acclimatization (Bradford et al., 2019) or substrate depletion. Yet, it still remains uncertain whether this subsoil-carbon loss will be sustained in the longer-term after 9.5 years of whole-soil experimental warming.

4.1.2 PCA indicated a possible shift in subsoil carbon composition

Soil carbon composition displayed marked changes with depth, with a decrease in aliphatic C–H and an increase in aromatic bonds, which is consistent with numerous studies (Chen et al., 2018; Kögel-Knabner, 2002; Rumpel et al., 2002; Schöning and Kögel-Knabner, 2006). After nearly-decadal warming, soils above 40 cm showed no clear SOC compositional shifts (Fig. 3), consistent with proportional area under the curve (AUC) contributions (Table S6) and unaltered DRIFT stability indices (DSI; Fig. 5) between treatments. Conversely, subsoil (below 40 cm) SOC composition tended to shift in the PCA plot towards lignin-like residues under warming (Fig. 3). We interpret this pattern cautiously as a multivariate compositional tendency, rather than as a statistically confirmed shift in specific bond types.

At 40–50 cm, the increased bulk lignin-like signal coincided with a stronger representation of lignin-like and aromatic C–H signals (range 2) in fPOM (Fig. S2). This pattern is further supported by significant increase in lignin-like ($p = 0.002$) and marginal increase in aromatic C–H AUC values (range 2; $p = 0.061$), both of which are associated with lignin-like compounds (Zaccheo et al., 2002). Because fPOM comprised nearly 40 % of total SOC at this depth (Fig. 2), compositional changes in this pool could be particularly important for the bulk soil signal. Below 50 cm, the corresponding pattern appeared to align more closely with a directional shift of most MAOM samples in warmed plots towards lignin-like signals (Fig. 3). However, there was high variability among replicates at these depths, likely due to spatial heterogeneity, and this trend should be therefore interpreted with caution.

4.2 Divergent roles of different density fractions for carbon sequestration

4.2.1 fPOM as a dynamic pool of soil carbon

The fPOM is typically assumed to exhibit the strongest response to warming, due to its lack of physical protection and thus high accessibility for microorganisms and the necessary components of efficient decomposition (Heckman et al., 2022; Lavallee et al., 2020; Rocci et al., 2021). However, our results demonstrated that the response of fPOM to warming vary with soil depth at our site, and the fraction was not quantitatively altered by warming in soils above 50 cm. Several site-specific factors likely attenuate accelerated fPOM decomposition under warming in the top 50 cm. Firstly, the fPOM in topsoils is more easily replenished by both aboveground and belowground inputs due to its proximity to vegetation (Angst et al., 2016). Second, the quality of the inputs may also contribute to these observed patterns. Mixed-coniferous litter typically has a high C : N ratio and lignin content (Silver and Miya, 2001), which can lower microbial carbon use efficiency (Manzoni et al., 2012). Consistent with this, fPOM at Blodgett Forest is N-poor with high C : N ratios (> 50 cm; Table S8; Soong et al., 2021). Finally, warming-induced topsoil drying (Pegoraro et al., 2026; Riley et al., 2025) likely inhibits microbial activity, particularly during summer drying season (Soong et al., 2021), thereby constraining decomposition and contributing to the unaltered fPOM quantity in the surface samples. Cumulatively, these factors suggest that continuous replenishment and environmentally constrained decomposition buffer fPOM against warming-induced losses in the soils above 50 cm despite the higher temperature sensitivity of this fraction.

Conversely, deep soil fPOM at 80–90 cm proved highly vulnerable. This deep fPOM quantitative loss was previously linked to enhanced microbial activity (Ofiti et al., 2021; Soong et al., 2021) and increased relative abundance of Actinobacteria (Zosso et al., 2021). This group of bacteria is known to utilize complex carbon (Barret et al., 2011; Goodfellow and Williams, 1983). Additionally, since 80 % of root biomass resides in the top 30 cm (Hicks Pries et al., 2017), depleted substrates and a lack of fresh plant inputs could exacerbate this deep soil fPOM decline.

The high sensitivity of this fraction is supported by its distinct depth-specific chemical composition shifts in response to warming. Specifically, fPOM composition was not affected in topsoils (Fig. S1), but it exhibited significant relative lignin-like enrichment, a tendency of increasing C / N ratios, and lower DSI and $\delta^{13}C$ values in mid-depth (Figs. S8 and S9). At 80–90 cm, very low fPOM recovery in the warmed plots precluded compositional analysis. However, the near absence of fPOM in the warmed subsoil further supports continued and disproportionate losses of this fraction under warming (Soong et al., 2021). Overall, these findings suggest that deep-soil fPOM represents a highly temperature-sensitive carbon pool where enhanced microbial decomposition is not balanced by new plant-derived inputs.

4.2.2 oPOM is equally dynamic, but a small pool at Blodgett

The oPOM fractions exhibited a similar depth-specific response to warming as fPOM (Fig. 1). Soong et al. (2021) found no significant reduction in oPOM throughout the soil profile, including the 80–90 cm interval. However, our results displayed consistently proportional reduction across soil depth and quantitatively significant loss at 80–90 cm (Figs. 1 and 2). We speculate that decadal warming might have destabilized aggregates and occluded SOC in the subsoil through time, supporting observations from a previous study (Poeplau et al., 2020). However, in contrast to fPOM, oPOM represented the smallest density fraction by mass and proportionally in our dataset, which was consistent with previous observations from Blodgett (Hicks Pries et al., 2017; Soong et al., 2021) and other studies (Schnecker et al., 2016; Schrumpf et al., 2013). Thus, despite evidence that warming may destabilize oPOM, the small size of this fraction indi-

cates that its contribution to warming-induced bulk SOC loss at Blodgett Forest is limited.

The SOC composition of oPOM was highly heterogeneous and showed no clear trends with depth or warming. This is evident in the wide spread of oPOM compositions along PC1 and PC2 (Fig. S2), reflecting the heterogeneity of SOC preserved by aggregates (Wagai et al., 2009; Wiesenberg et al., 2010). This heterogeneity likely arises because oPOM comprises a mixture of POM with different origins, decomposition states, and residence times (Dorodnikov et al., 2011; Wiesenberg et al., 2010). As particulate material becomes occluded into aggregates of varying stability, it experiences differing degrees of physical protection, microbial processing, and turnover, resulting a broader range in $\delta^{13}C$ and $\Delta^{14}C$ values (Marín-Spiotta et al., 2008; McFarlane et al., 2013; Rowley et al., 2021; Schrumpf et al., 2013). Yet, overall while oPOM was heterogeneous and its sensitivity to warming may have increased with time to reflect changes in fPOM, it was a quantitatively small pool of SOC at Blodgett Forest.

4.2.3 Subsoil MAOM as a long-term carbon preservation pool

The mineral-associated organic matter was consistently less responsive to warming than fPOM and oPOM across the soil profile (Figs. 1 and 2). Our results provide among the first fraction-resolved evidence that subsoil MAOM remained stable in both mass and chemical composition under nearly-decadal whole-soil warming. This pattern aligns with other warming studies (Schindlbacher et al., 2009; Schnecker et al., 2016) but contrasts with Chen et al. (2023), who documented warming-induced significant MAOM loss. In our warmed topsoils, we hypothesize that greater plant inputs (Castellano et al., 2015) combined with warming-elevated microbial activity could have offset MAOM destabilization and loss (Cotrufo et al., 2013; Islam et al., 2022), resulting in constant MAOM. In our deep subsoils (> 50 cm), we hypothesized that MAOM remains stable likely because the accelerated decomposition of fPOM and oPOM provided substrates that were subsequently adsorbed to mineral surfaces. Another possible reason would be that warming can also enhance vertical transport of dissolved organic matter (Soong et al., 2021), which can be efficiently associated with minerals (Kramer et al., 2012; Mikutta et al., 2019; Villarino et al., 2021; Yu et al., 2022). This apparent stability of MAOM stocks under warming is further supported by its largely unchanged chemical composition and on average increased DSI in subsoils.

MAOM composition remained consistent in subsoils under warming, characterized mainly by both C=C aromatic (range 2) and lignin-like peaks (Table S8), a pattern not observed in the bulk soil (Fig. 3). This supports the substantial loss of C=C aromatic compounds (range 2) from fPOM under warming and aligns with significant loss of aromatic polymers documented at this site (Zosso et al., 2023). Although such compounds are typically considered chemically complex and were previously thought to accumulate during microbial decomposition (Calderón et al., 2013; Demyan et al., 2012; Haberhauer et al., 1998), their decline suggests that mineral protection rather than intrinsic recalcitrance governs SOC persistence (Marschner et al., 2008). Organo-mineral associations may account for the pronounced lignin-like signal and higher average DSI in warmed deep soil, as phenolic-rich lignin derivatives are readily stabilized by different geochemical actors (Kögel-Knabner et al., 2008; Rowley et al., 2025). Collectively, the small changes in its concentration and composition support the notion that MAOM is a slow-cycling carbon pool at Blodgett, which buffers soil carbon loss under nearly-decadal whole-soil warming.

5 Conclusion

Our study is the first to investigate the SOC composition across different soil fractions within a whole-soil field warming experiment after 9.5 years of warming. Our findings highlight that bulk soil and SOC fractions responded differently to long-term warming, with fPOM and oPOM being more responsive than MAOM over a nearly-decadal timescale. The loss of dynamic fPOM fraction in part drives the consistent decrease in SOC concentrations at certain depths in subsoil. This has direct implications for carbon-climate feedback modeling, as initial warming-enhanced CO_2 fluxes (Hicks Pries et al., 2017; Soong et al., 2021) may be attenuated over decadal timescales by the depletion of this labile POM in the subsoil. MAOM showed much lower responses to warming than the POM fraction, and was enriched in aromatic and lignin-like compounds. We demonstrate that combining DRIFT spectroscopy with density fractionation provides a more powerful approach for better understanding SOC dynamics under warming than analyzing bulk soil alone. Future whole-soil warming experiments should prioritize studying the responses of subsoils and distinct SOC fractions to better resolve depth-specific carbon dynamics and improve predictions of soil carbon–climate feedbacks.

Code and data availability. All data from this study is available on ESS-Dive (https://doi.org/10.15485/3024414, Sun et al., 2026).

Supplement. The supplement related to this article is available online at https://doi.org/10.5194/soil-12-757-2026-supplement.

Author contributions. BS conducted all the lab work, contributed to field work, wrote the original draft, conducted statistical analysis, and created the figures. GLBW supervised BS, contributed to methods, conceptualization, data interpretation and validation, edited, and reviewed the manuscript. MWIS obtained funding for Zurich costs, and contributed to conceptualization, data interpreta-

tion, writing reviews, and editing. EP led the field work, and contributed to statistical analysis, writing review. MST designed and is PI of the Blodgett whole-soil warming experiment, contributed to field work, and edited the manuscript. MCR developed the DRIFT spectra analysis pipeline for spectral analysis and calculation, contributed to statistical analysis, conceptualization, data interpretation and validation, edited and reviewed the manuscript.

Competing interests. The contact author has declared that none of the authors has any competing interests.

Disclaimer. Publisher's note: Copernicus Publications remains neutral with regard to jurisdictional claims made in the text, published maps, institutional affiliations, or any other geographical representation in this paper. The authors bear the ultimate responsibility for providing appropriate place names. Views expressed in the text are those of the authors and do not necessarily reflect the views of the publisher.

Acknowledgements. We thank Jan Pfiffner, Julia van Leeuwen, Thomas Keller, Barbara Siegfried, and Yves Brügger for support with laboratory analyses. We thank Cristina Castanha and Niklas Blanadet for support with field work and Rachel C. Porras for training with density fractionation.

Financial support. This research has been supported by the Schweizerischer Nationalfonds zur Förderung der Wissenschaftlichen Forschung (grant no. 200021_172744) and the US Department of Energy (grant no. DE–AC02–05CH11231).

Review statement. This paper was edited by Hu Zhou and reviewed by Hayley Peter-Contesse and one anonymous referee.

References

Akaike, H.: Information Theory and an Extension of the Maximum Likelihood Principle, in: Selected Papers of Hirotugu Akaike, edited by: Parzen, E., Tanabe, K., and Kitagawa, G., Springer, New York, NY, 199–213, https://doi.org/10.1007/978-1-4612-1694-0_15, 1998.

Angst, G., John, S., Mueller, C. W., Kögel-Knabner, I., and Rethemeyer, J.: Tracing the sources and spatial distribution of organic carbon in subsoils using a multi-biomarker approach, Sci. Rep., 6, 29478, https://doi.org/10.1038/srep29478, 2016.

Angst, G., Mueller, K. E., Nierop, K. G. J., and Simpson, M. J.: Plant- or microbial-derived? A review on the molecular composition of stabilized soil organic matter, Soil Biol. Biochem., 156, 108189, https://doi.org/10.1016/j.soilbio.2021.108189, 2021.

Artz, R. R. E., Chapman, S. J., Jean Robertson, A. H., Potts, J. M., Laggoun-Défarge, F., Gogo, S., Comont, L., Disnar, J.-R., and Francez, A.-J.: FTIR spectroscopy can be used as a screening tool for organic matter quality in regenerating cutover peatlands, Soil Biol. Biochem., 40, 515–527, https://doi.org/10.1016/j.soilbio.2007.09.019, 2008.

Barret, M., Morrissey, J. P., and O'Gara, F.: Functional genomics analysis of plant growth-promoting rhizobacterial traits involved in rhizosphere competence, Biol. Fertil. Soils, 47, 729–743, https://doi.org/10.1007/s00374-011-0605-x, 2011.

Bradford, M. A., McCulley, R. L., Crowther, T. W., Oldfield, E. E., Wood, S. A., and Fierer, N.: Cross-biome patterns in soil microbial respiration predictable from evolutionary theory on thermal adaptation, Nat. Ecol. Evol., 3, 223–231, https://doi.org/10.1038/s41559-018-0771-4, 2019.

Button, E. S., Pett-Ridge, J., Murphy, D. V., Kuzyakov, Y., Chadwick, D. R., and Jones, D. L.: Deep-C storage: Biological, chemical and physical strategies to enhance carbon stocks in agricultural subsoils, Soil Biol. Biochem., 170, 108697, https://doi.org/10.1016/j.soilbio.2022.108697, 2022.

Calderón, F., Haddix, M., Conant, R., Magrini-Bair, K., and Paul, E.: Diffuse-reflectance Fourier-transform mid-infrared spectroscopy as a method of characterizing changes in soil organic matter, Soil Sci. Soc. Am. J., 77, 1591–1600, https://doi.org/10.2136/sssaj2013.04.0131, 2013.

Castellano, M. J., Mueller, K. E., Olk, D. C., Sawyer, J. E., and Six, J.: Integrating plant litter quality, soil organic matter stabilization, and the carbon saturation concept, Global Change Biol., 21, 3200–3209, https://doi.org/10.1111/gcb.12982, 2015.

Chatterjee, S., Santos, F., Abiven, S., Itin, B., Stark, R. E., and Bird, J. A.: Elucidating the chemical structure of pyrogenic organic matter by combining magnetic resonance, mid-infrared spectroscopy and mass spectrometry, Org. Geochem., 51, 35–44, https://doi.org/10.1016/j.orggeochem.2012.07.006, 2012.

Chen, C., Leinweber, P., Eckhardt, K.-U., and Sparks, D. L.: The composition and stability of clay-associated organic matter along a soil profile, Soil Syst., 2, 16, https://doi.org/10.3390/soilsystems2010016, 2018.

Chen, Y., Han, M., Yuan, X., Zhou, H., Zhao, X., Schimel, J. P., and Zhu, B.: Long-term warming reduces surface soil organic carbon by reducing mineral-associated carbon rather than "free" particulate carbon, Soil Biol. Biochem., 177, 108905, https://doi.org/10.1016/j.soilbio.2022.108905, 2023.

Coplen, T. B.: Guidelines and recommended terms for expression of stable-isotope-ratio and gas-ratio measurement results, Rapid Commun. Mass Spectrom., 25, 2538–2560, https://doi.org/10.1002/rcm.5129, 2011.

Cotrufo, M. F., Wallenstein, M. D., Boot, C. M., Denef, K., and Paul, E.: The Microbial Efficiency-Matrix Stabilization (MEMS) framework integrates plant litter decomposition with soil organic matter stabilization: do labile plant inputs form stable soil organic matter?, Global Change Biol., 19, 988–995, https://doi.org/10.1111/gcb.12113, 2013.

Davidson, E. A. and Janssens, I. A.: Temperature sensitivity of soil carbon decomposition and feedbacks to climate change, Nature, 440, 165–173, https://doi.org/10.1038/nature04514, 2006.

Demyan, M. S., Rasche, F., Schulz, E., Breulmann, M., Müller, T., and Cadisch, G.: Use of specific peaks obtained by diffuse reflectance Fourier transform mid-infrared spectroscopy to study the composition of organic matter in a Haplic Chernozem, Eur. J. Soil Sci., 63, 189–199, https://doi.org/10.1111/j.1365-2389.2011.01420.x, 2012.

Dorodnikov, M., Kuzyakov, Y., Fangmeier, A., and Wiesenberg, G. L. B.: C and N in soil organic matter density fractions under elevated atmospheric CO_2: Turnover vs. stabilization, Soil Biol. Biochem., 43, 579–589, https://doi.org/10.1016/j.soilbio.2010.11.026, 2011.

Ellerbrock, R. H. and Gerke, H. H.: FTIR spectral band shifts explained by OM–cation interactions, J. Plant Nutr. Soil Sci., 184, 388–397, https://doi.org/10.1002/jpln.202100056, 2021.

Fearn, T.: The interaction between standard normal variate and derivatives, NIR News, 19, 16–17, https://doi.org/10.1255/nirn.1098, 2008.

Georgiou, K., Jackson, R. B., Vindušková, O., Abramoff, R. Z., Ahlström, A., Feng, W., Harden, J. W., Pellegrini, A. F. A., Polley, H. W., Soong, J. L., Riley, W. J., and Torn, M. S.: Global stocks and capacity of mineral-associated soil organic carbon, Nat. Commun., 13, 3797, https://doi.org/10.1038/s41467-022-31540-9, 2022.

Georgiou, K., Koven, C. D., Wieder, W. R., Hartman, M. D., Riley, W. J., Pett-Ridge, J., Bouskill, N. J., Abramoff, R. Z., Slessarev, E. W., Ahlström, A., Parton, W. J., Pellegrini, A. F. A., Pierson, D., Sulman, B. N., Zhu, Q., and Jackson, R. B.: Emergent temperature sensitivity of soil organic carbon driven by mineral associations, Nat. Geosci., 17, 205–212, https://doi.org/10.1038/s41561-024-01384-7, 2024.

Giardina, C. P., Litton, C. M., Crow, S. E., and Asner, G. P.: Warming-related increases in soil CO_2 efflux are explained by increased below-ground carbon flux, Nat. Clim. Change, 4, 822–827, https://doi.org/10.1038/nclimate2322, 2014.

Golchin, A., Oades, J., Skjemstad, J., and Clarke, P.: Study of free and occluded particulate organic matter in soils by solid state ^{13}C Cp/MAS NMR spectroscopy and scanning electron microscopy, Soil Res., 32, 285, https://doi.org/10.1071/SR9940285, 1994.

Goodfellow, M. and Williams, S. T.: Ecology of Actinomycetes, Annu. Rev. Microbiol., 37, 189–216, https://doi.org/10.1146/annurev.mi.37.100183.001201, 1983.

Grand, S., Hudson, R., and Lavkulich, L. M.: Effects of forest harvest on soil nutrients and labile ions in Podzols of southwestern Canada: Mean and dispersion effects, Catena, 122, 18–26, https://doi.org/10.1016/j.catena.2014.06.004, 2014.

Guan, S., An, N., Zong, N., He, Y., Shi, P., Zhang, J., and He, N.: Climate warming impacts on soil organic carbon fractions and aggregate stability in a Tibetan alpine meadow, Soil Biol. Biochem., 116, 224–236, https://doi.org/10.1016/j.soilbio.2017.10.011, 2018.

Haberhauer, G., Rafferty, B., Strebl, F., and Gerzabek, M. H.: Comparison of the composition of forest soil litter derived from three different sites at various decompositional stages using FTIR spectroscopy, Geoderma, 83, 331–342, https://doi.org/10.1016/S0016-7061(98)00008-1, 1998.

Harrison, R. B., Footen, P. W., and Strahm, B. D.: Deep Soil Horizons: Contribution and importance to soil carbon pools and in assessing whole-ecosystem response to management and global change, Forest. Sci., 57, 67–76, https://doi.org/10.1093/forestscience/57.1.67, 2011.

Heckman, K., Hicks Pries, C. E., Lawrence, C. R., Rasmussen, C., Crow, S. E., Hoyt, A. M., von Fromm, S. F., Shi, Z., Stoner, S., McGrath, C., Beem-Miller, J., Berhe, A. A., Blankinship, J. C., Keiluweit, M., Marín-Spiotta, E., Monroe, J. G., Plante, A. F., Schimel, J., Sierra, C. A., Thompson, A., and Wagai, R.: Beyond bulk: Density fractions explain heterogeneity in global soil carbon abundance and persistence, Global Change Biol., 28, 1178–1196, https://doi.org/10.1111/gcb.16023, 2022.

Hicks Pries, C., Ryals, R., Zhu, B., Min, K., Cooper, A., Goldsmith, S., Pett-Ridge, J., Torn, M., and Asefaw Berhe, A.: The deep soil organic carbon response to global change, Annu. Rev. Ecol. Evol. Syst., 54, https://doi.org/10.1146/annurev-ecolsys-102320-085332, 2023.

Hicks Pries, C. E., Castanha, C., Porras, R. C., and Torn, M. S.: The whole–soil carbon flux in response to warming, Science, 355, 1420–1423, https://doi.org/10.1126/science.aal1319, 2017.

Hicks Pries, C. E., Sulman, B. N., West, C., O'Neill, C., Poppleton, E., Porras, R. C., Castanha, C., Zhu, B., Wiedemeier, D. B., and Torn, M. S.: Root litter decomposition slows with soil depth, Soil Biol. Biochem., 125, 103–114, https://doi.org/10.1016/j.soilbio.2018.07.002, 2018.

Husson, F., Lê, S., and Pagès, J.: Confidence ellipse for the sensory profiles obtained by principal component analysis, Food Qual. Prefer., 16, 245–250, https://doi.org/10.1016/j.foodqual.2004.04.019, 2005.

IPCC: Climate Change 2023: Synthesis Report, in: Contribution of Working Groups I, II and III to the Sixth Assessment Report of the Intergovernmental Panel on Climate Change, edited by: Lee, H. and Romero, J., IPCC, Geneva, Switzerland, 35–115, https://doi.org/10.59327/IPCC/AR6-9789291691647, 2023.

Islam, M. R., Singh, B., and Dijkstra, F. A.: Stabilisation of soil organic matter: Interactions between clay and microbes, Biogeochemistry, 160, 145–158, https://doi.org/10.1007/s10533-022-00956-2, 2022.

IUSS Working Group WRB: World Reference Base for Soil Resources, International soil classification system for naming soils and creating legends for soil maps, in: 4th Edn., IUSS – International Union of Soil Sciences, Vienna, Austria, https://wrb.isric.org/documents.html (last access: 2 July 2026), 2022.

Jackson, R. B., Canadell, J., Ehleringer, J. R., Mooney, H. A., Sala, O. E., and Schulze, E. D.: A global analysis of root distributions for terrestrial biomes, Oecologia, 108, 389–411, https://doi.org/10.1007/BF00333714, 1996.

Jackson, R. B., Lajtha, K., Crow, S. E., Hugelius, G., Kramer, M. G., and Piñeiro, G.: The ecology of soil carbon: Pools, vulnerabilities, and biotic and abiotic controls, Annu. Rev. Ecol. Evol. Syst., 48, 419–445, https://doi.org/10.1146/annurev-ecolsys-112414-054234, 2017.

Jobbágy, E. G. and Jackson, R. B.: The vertical distribution of soil organic carbon and its relation to climate and vegetation, Ecol. Appl., 10, 423–436, https://doi.org/10.1890/1051-0761(2000)010[0423:TVDOSO]2.0.CO;2, 2000.

Kaiser, K. and Guggenberger, G.: The role of DOM sorption to mineral surfaces in the preservation of organic matter in soils, Org. Geochem., 31, 711–725, https://doi.org/10.1016/S0146-6380(00)00046-2, 2000.

Kleber, M., Bourg, I. C., Coward, E. K., Hansel, C. M., Myneni, S. C. B., and Nunan, N.: Dynamic interactions at the mineral–organic matter interface, Nat. Rev. Earth Environ., 2, 402–421, https://doi.org/10.1038/s43017-021-00162-y, 2021.

Kögel-Knabner, I.: The macromolecular organic composition of plant and microbial residues as inputs to soil organic matter, Soil

Biol. Biochem., 34, 139–162, https://doi.org/10.1016/S0038-0717(01)00158-4, 2002.

Kögel-Knabner, I., Guggenberger, G., Kleber, M., Kandeler, E., Kalbitz, K., Scheu, S., Eusterhues, K., and Leinweber, P.: Organo-mineral associations in temperate soils: Integrating biology, mineralogy, and organic matter chemistry, J. Plant Nutr. Soil Sci., 171, 61–82, https://doi.org/10.1002/jpln.200700048, 2008.

Kramer, M. G., Sanderman, J., Chadwick, O. A., Chorover, J., and Vitousek, P. M.: Long-term carbon storage through retention of dissolved aromatic acids by reactive particles in soil, Global Change Biol., 18, 2594–2605, https://doi.org/10.1111/j.1365-2486.2012.02681.x, 2012.

Kwatcho Kengdo, S., Peršoh, D., Schindlbacher, A., Heinzle, J., Tian, Y., Wanek, W., and Borken, W.: Long-term soil warming alters fine root dynamics and morphology, and their ectomycorrhizal fungal community in a temperate forest soil, Global Change Biol., 28, 3441–3458, https://doi.org/10.1111/gcb.16155, 2022.

Laub, M., Demyan, M. S., Nkwain, Y. F., Blagodatsky, S., Kätterer, T., Piepho, H.-P., and Cadisch, G.: DRIFTS band areas as measured pool size proxy to reduce parameter uncertainty in soil organic matter models, Biogeosciences, 17, 1393–1413, https://doi.org/10.5194/bg-17-1393-2020, 2020.

Lavallee, J. M., Soong, J. L., and Cotrufo, M. F.: Conceptualizing soil organic matter into particulate and mineral-associated forms to address global change in the 21st century, Global Change Biol., 26, 261–273, https://doi.org/10.1111/gcb.14859, 2020.

Lehmann, J. and Kleber, M.: The contentious nature of soil organic matter, Nature, 528, 60–68, https://doi.org/10.1038/nature16069, 2015.

Lu, M., Zhou, X., Yang, Q., Li, H., Luo, Y., Fang, C., Chen, J., Yang, X., and Li, B.: Responses of ecosystem carbon cycle to experimental warming: a meta-analysis, Ecology, 94, 726–738, https://doi.org/10.1890/12-0279.1, 2013.

Lugato, E., Lavallee, J. M., Haddix, M. L., Panagos, P., and Cotrufo, M. F.: Different climate sensitivity of particulate and mineral-associated soil organic matter, Nat. Geosci., 14, 295–300, https://doi.org/10.1038/s41561-021-00744-x, 2021.

Manzoni, S., Taylor, P., Richter, A., Porporato, A., and Ågren, G. I.: Environmental and stoichiometric controls on microbial carbon-use efficiency in soils, New Phytol., 196, 79–91, https://doi.org/10.1111/j.1469-8137.2012.04225.x, 2012.

Marín-Spiotta, E., Swanston, C. W., Torn, M. S., Silver, W. L., and Burton, S. D.: Chemical and mineral control of soil carbon turnover in abandoned tropical pastures, Geoderma, 143, 49–62, https://doi.org/10.1016/j.geoderma.2007.10.001, 2008.

Marschner, B., Brodowski, S., Dreves, A., Gleixner, G., Gude, A., Grootes, P. M., Hamer, U., Heim, A., Jandl, G., Ji, R., Kaiser, K., Kalbitz, K., Kramer, C., Leinweber, P., Rethemeyer, J., Schäffer, A., Schmidt, M. W. I., Schwark, L., and Wiesenberg, G. L. B.: How relevant is recalcitrance for the stabilization of organic matter in soils?, J. Plant Nutr. Soil Sci., 171, 91–110, https://doi.org/10.1002/jpln.200700049, 2008.

McFarlane, K. J., Torn, M. S., Hanson, P. J., Porras, R. C., Swanston, C. W., Callaham, M. A., and Guilderson, T. P.: Comparison of soil organic matter dynamics at five temperate deciduous forests with physical fractionation and radiocarbon measurements, Biogeochemistry, 112, 457–476, https://doi.org/10.1007/s10533-012-9740-1, 2013.

Mikutta, R., Turner, S., Schippers, A., Gentsch, N., Meyer-Stüve, S., Condron, L. M., Peltzer, D. A., Richardson, S. J., Eger, A., Hempel, G., Kaiser, K., Klotzbücher, T., and Guggenberger, G.: Microbial and abiotic controls on mineral-associated organic matter in soil profiles along an ecosystem gradient, Sci. Rep., 9, 10294, https://doi.org/10.1038/s41598-019-46501-4, 2019.

North, P. F.: Towards an Absolute Measurement of Soil Structural Stability Using Ultrasound, J. Soil Sci., 27, 451–459, https://doi.org/10.1111/j.1365-2389.1976.tb02014.x, 1976.

Nottingham, A. T., Meir, P., Velasquez, E., and Turner, B. L.: Soil carbon loss by experimental warming in a tropical forest, Nature, 584, 234–237, https://doi.org/10.1038/s41586-020-2566-4, 2020.

Ofiti, N. O. E., Zosso, C. U., Soong, J. L., Solly, E. F., Torn, M. S., Wiesenberg, G. L. B., and Schmidt, M. W. I.: Warming promotes loss of subsoil carbon through accelerated degradation of plant-derived organic matter, Soil Biol. Biochem., 156, 108185, https://doi.org/10.1016/j.soilbio.2021.108185, 2021.

Pegoraro, E., Zosso, C. U., Wiesenberg, G. L. B., Castanha, C., Hicks Pries, C. E., Porras, R. C., Soong, J. L., Schmidt, M. W. I., and Torn, M. S.: The depth-dependent microbial response to root litter input in an experimental whole-soil warming study, Soil Biol. Biochem., 216, 110106, https://doi.org/10.1016/j.soilbio.2026.110106, 2026.

Pinheiro, J., Bates, D., and R Core Team: nlme: Linear and nonlinear mixed effects models, R package version 3.1-168, CRAN, https://doi.org/10.32614/CRAN.package.nlme, 2025.

Pinheiro, J. C. and Bates, D. M.: Mixed-effects models in S and S-PLUS, Springer, New York, https://doi.org/10.1007/b98882, 2000.

Poeplau, C., Sigurðsson, P., and Sigurdsson, B. D.: Depletion of soil carbon and aggregation after strong warming of a subarctic Andosol under forest and grassland cover, SOIL, 6, 115–129, https://doi.org/10.5194/soil-6-115-2020, 2020.

Posit team: RStudio: Integrated Development Environment for R (Version 2024.12.1.563), Posit Software, PBC, Boston, MA, https://posit.co/ (last access: 1 July 2026), 2024.

R Core Team: R: A language and environment for statistical computing, R Foundation for Statistical Computing, Vienna, Austria, https://www.R-project.org/ (last access: 1 July 2026), 2025.

Reeves, J. B.: Mid-infrared spectral interpretation of soils: Is it practical or accurate?, Geoderma, 189–190, 508–513, https://doi.org/10.1016/j.geoderma.2012.06.008, 2012.

Riley, W. J., Tao, J., Mekonnen, Z. A., Grant, R. F., Brodie, E. L., Pegoraro, E., and Torn, M. S.: Experimental soil warming impacts soil moisture and plant water stress and thereby ecosystem carbon dynamics, J. Adv. Model. Earth Syst., 17, e2024MS004714, https://doi.org/10.1029/2024MS004714, 2025.

Rocci, K. S., Lavallee, J. M., Stewart, C. E., and Cotrufo, M. F.: Soil organic carbon response to global environmental change depends on its distribution between mineral-associated and particulate organic matter: A meta-analysis, Sci. Total Environ., 793, 148569, https://doi.org/10.1016/j.scitotenv.2021.148569, 2021.

Rowley, M. C., Grand, S., Spangenberg, J. E., and Verrecchia, E. P.: Evidence linking calcium to increased organo-mineral association in soils, Biogeochemistry, 153, 223–241, https://doi.org/10.1007/s10533-021-00779-7, 2021.

Rowley, M. C., Pena, J., Marcus, M. A., Porras, R., Pegoraro, E., Zosso, C., Ofiti, N. O. E., Wiesenberg, G. L. B., Schmidt, M. W. I., Torn, M. S., and Nico, P. S.: Calcium is associated with specific soil organic carbon decomposition products, SOIL, 11, 381–388, https://doi.org/10.5194/soil-11-381-2025, 2025.

Rumpel, C., Kögel-Knabner, I., and Bruhn, F.: Vertical distribution, age, and chemical composition of organic carbon in two forest soils of different pedogenesis, Org. Geochem., 33, 1131–1142, https://doi.org/10.1016/S0146-6380(02)00088-8, 2002.

Sanderman, J., Maddern, T., and Baldock, J.: Similar composition but differential stability of mineral retained organic matter across four classes of clay minerals, Biogeochemistry, 121, 409–424, https://doi.org/10.1007/s10533-014-0009-8, 2014.

Savitzky, A. and Golay, M. J. E.: Smoothing and Differentiation of Data by Simplified Least Squares Procedures, Anal. Chem., 36, 1627–1639, https://doi.org/10.1021/ac60214a047, 1964.

Scharlemann, J. P., Tanner, E. V., Hiederer, R., and Kapos, V.: Global soil carbon: understanding and managing the largest terrestrial carbon pool, Carbon Manage., 5, 81–91, https://doi.org/10.4155/cmt.13.77, 2014.

Schiedung, M., Barré, P., and Peoplau, C.: Separating fast from slow cycling soil organic carbon – A multi-method comparison on land use change sites, Geoderma, 453, 117154, https://doi.org/10.1016/j.geoderma.2024.117154, 2025.

Schindlbacher, A., Zechmeister-Boltenstern, S., and Jandl, R.: Carbon losses due to soil warming: Do autotrophic and heterotrophic soil respiration respond equally?, Global Change Biol., 15, 901–913, https://doi.org/10.1111/j.1365-2486.2008.01757.x, 2009.

Schlesinger, W. H.: Evidence from chronosequence studies for a low carbon-storage potential of soils, Nature, 348, 232–234, https://doi.org/10.1038/348232a0, 1990.

Schlesinger, W. H. and Andrews, J. A.: Soil respiration and the global carbon cycle, Biogeochemistry, 48, 7–20, https://doi.org/10.1023/A:1006247623877, 2000.

Schnecker, J., Borken, W., Schindlbacher, A., and Wanek, W.: Little effects on soil organic matter chemistry of density fractions after seven years of forest soil warming, Soil Biol. Biochem., 103, 300–307, https://doi.org/10.1016/j.soilbio.2016.09.003, 2016.

Schöning, I. and Kögel-Knabner, I.: Chemical composition of young and old carbon pools throughout Cambisol and Luvisol profiles under forests, Soil Biol. Biochem., 38, 2411–2424, https://doi.org/10.1016/j.soilbio.2006.03.005, 2006.

Schrumpf, M., Kaiser, K., Guggenberger, G., Persson, T., Kögel-Knabner, I., and Schulze, E.-D.: Storage and stability of organic carbon in soils as related to depth, occlusion within aggregates, and attachment to minerals, Biogeosciences, 10, 1675–1691, https://doi.org/10.5194/bg-10-1675-2013, 2013.

Silver, W. L. and Miya, R. K.: Global patterns in root decomposition: comparisons of climate and litter quality effects, Oecologia, 129, 407–419, https://doi.org/10.1007/s004420100740, 2001.

Sollins, P., Glassman, C., Paul, E. A., Swanston, C., Lajtha, K., Heil, J. W., and Elliott, E. T.: Soil Carbon and Nitrogen Pools and Fractions, in: Standard Soil Methods for Long-term Ecological Research, edited by: Robertson, G. P., Coleman, D. C., Bledsoe, C. S., and Sollins, P., Oxford University Press, https://doi.org/10.1093/oso/9780195120837.003.0005, 1999.

Soong, J. L., Castanha, C., Hicks Pries, C. E., Ofiti, N., Porras, R. C., Riley, W. J., Schmidt, M. W. I., and Torn, M. S.: Five years of whole–soil warming led to loss of subsoil carbon stocks and increased CO_2 efflux, Sci. Adv., 7, eabd1343, https://doi.org/10.1126/sciadv.abd1343, 2021.

Spohn, M.: Preferential adsorption of nitrogen- and phosphorus-containing organic compounds to minerals in soils: A review, Soil Biol. Biochem., 194, 109428, https://doi.org/10.1016/j.soilbio.2024.109428, 2024.

Stevens, A. and Ramirez-Lopez, L.: prospectr: Miscellaneous functions for processing and sample selection of vis–NIR diffuse reflectance data, R package version 0.2.5, CRAN, https://doi.org/10.32614/CRAN.package.prospectr, 2025.

Sun, B., Wiesenberg, G., Pegoraro, E., Torn, M., Schmidt, M., and Rowley, M.: Effects of 9.5 years warming on SOC concentration and composition in bulk soil and density fractions. Belowground Biogeochemistry Scientific Focus Area, ESS-DIVE repository [data set], https://doi.org/10.15485/3024414, 2026.

Tinti, A., Tugnoli, V., Bonora, S., and Francioso, O.: Recent applications of vibrational mid-Infrared (IR) spectroscopy for studying soil components: a review, J. Cent. Eur. Agric., 16, 1–22, https://doi.org/10.5513/JCEA01/16.1.1535, 2015.

vandenEnden, L., Anthony, M. A., Frey, S. D., and Simpson, M. J.: Biogeochemical evolution of soil organic matter composition after a decade of warming and nitrogen addition, Biogeochemistry, 156, 161–175, https://doi.org/10.1007/s10533-021-00837-0, 2021.

Verbrigghe, N., Leblans, N. I. W., Sigurdsson, B. D., Vicca, S., Fang, C., Fuchslueger, L., Soong, J. L., Weedon, J. T., Poeplau, C., Ariza-Carricondo, C., Bahn, M., Guenet, B., Gundersen, P., Gunnarsdóttir, G. E., Kätterer, T., Liu, Z., Maljanen, M., Marañón-Jiménez, S., Meeran, K., Oddsdóttir, E. S., Ostonen, I., Peñuelas, J., Richter, A., Sardans, J., Sigurðsson, P., Torn, M. S., Van Bodegom, P. M., Verbruggen, E., Walker, T. W. N., Wallander, H., and Janssens, I. A.: Soil carbon loss in warmed subarctic grasslands is rapid and restricted to topsoil, Biogeosciences, 19, 3381–3393, https://doi.org/10.5194/bg-19-3381-2022, 2022.

Villarino, S. H., Pinto, P., Jackson, R. B., and Piñeiro, G.: Plant rhizodeposition: A key factor for soil organic matter formation in stable fractions, Sci. Adv., 7, eabd3176, https://doi.org/10.1126/sciadv.abd3176, 2021.

von Lützow, M., Kögel-Knabner, I., Ekschmitt, K., Matzner, E., Guggenberger, G., Marschner, B., and Flessa, H.: Stabilization of organic matter in temperate soils: Mechanisms and their relevance under different soil conditions – a review, Eur. J. Soil Sci., 57, 426–445, https://doi.org/10.1111/j.1365-2389.2006.00809.x, 2006.

Vu, V. Q. and Friendly, M.: ggbiplot: A grammar of graphics implementation of biplots, R package version 0.6.2, CRAN, https://doi.org/10.32614/CRAN.package.ggbiplot, 2024.

Wagai, R., Mayer, L. M., and Kitayama, K.: Nature of the "occluded" low-density fraction in soil organic matter studies: A critical review, Soil Sci. Plant Nutr., 55, 13–25, https://doi.org/10.1111/j.1747-0765.2008.00356.x, 2009.

Wickham, H.: ggplot2: Elegant graphics for data analysis, in: 2nd Edn., Springer-Verlag, New York, https://doi.org/10.1007/978-3-319-24277-4, 2016.

Wickham, H., Averick, M., Bryan, J., Chang, W., McGowan, L. D., François, R., Grolemund, G., Hayes, A., Henry, L., Hester, J., Kuhn, M., Pedersen, T. L., Miller, E., Bache, S. M., Müller, K., Ooms, J., Robinson, D., Seidel, D. P., Spinu, V., Takahashi, K., Vaughan, D., Wilke, C., Woo, K., and Yutani,

H.: Welcome to the tidyverse, J. Open Sour. Softw., 4, 1686, https://doi.org/10.21105/joss.01686, 2019.

Wiesenberg, G. L. B., Dorodnikov, M., and Kuzyakov, Y.: Source determination of lipids in bulk soil and soil density fractions after four years of wheat cropping, Geoderma, 156, 267–277, https://doi.org/10.1016/j.geoderma.2010.02.026, 2010.

Williams, E. K., Fogel, M. L., Berhe, A. A., and Plante, A. F.: Distinct bioenergetic signatures in particulate versus mineral-associated soil organic matter, Geoderma, 330, 107–116, https://doi.org/10.1016/j.geoderma.2018.05.024, 2018.

Witzgall, K., Vidal, A., Schubert, D. I., Höschen, C., Schweizer, S. A., Buegger, F., Pouteau, V., Chenu, C., and Mueller, C. W.: Particulate organic matter as a functional soil component for persistent soil organic carbon, Nat. Commun., 12, 4115, https://doi.org/10.1038/s41467-021-24192-8, 2021.

Wordell-Dietrich, P., Wotte, A., Rethemeyer, J., Bachmann, J., Helfrich, M., Kirfel, K., Leuschner, C., and Don, A.: Vertical partitioning of CO_2 production in a forest soil, Biogeosciences, 17, 6341–6356, https://doi.org/10.5194/bg-17-6341-2020, 2020.

Xu, Z. and Tsang, D. C. W.: Mineral-mediated stability of organic carbon in soil and relevant interaction mechanisms, Eco-Environ. Health, 3, 59–76, https://doi.org/10.1016/j.eehl.2023.12.003, 2024.

Yu, W., Huang, W., Weintraub-Leff, S. R., and Hall, S. J.: Where and why do particulate organic matter (POM) and mineral-associated organic matter (MAOM) differ among diverse soils?, Soil Biol. Biochem., 172, 108756, https://doi.org/10.1016/j.soilbio.2022.108756, 2022.

Zaccheo, P., Cabassi, G., Ricca, G., and Crippa, L.: Decomposition of organic residues in soil: experimental technique and spectroscopic approach, Org. Geochem., 33, 327–345, https://doi.org/10.1016/S0146-6380(01)00164-4, 2002.

Zosso, C. U., Ofiti, N. O. E., Soong, J. L., Solly, E. F., Torn, M. S., Huguet, A., Wiesenberg, G. L. B., and Schmidt, M. W. I.: Whole-soil warming decreases abundance and modifies the community structure of microorganisms in the subsoil but not in surface soil, SOIL, 7, 477–494, https://doi.org/10.5194/soil-7-477-2021, 2021.

Zosso, C. U., Ofiti, N. O. E., Torn, M. S., Wiesenberg, G. L. B., and Schmidt, M. W. I.: Rapid loss of complex polymers and pyrogenic carbon in subsoils under whole-soil warming, Nat. Geosci., 16, 344–348, https://doi.org/10.1038/s41561-023-01142-1, 2023.

Zuur, A. F., Ieno, E. N., Walker, N., Saveliev, A. A., and Smith, G. M.: Mixed effects models and extensions in ecology with R, Springer, New York, NY, https://doi.org/10.1007/978-0-387-87458-6, 2009.